

Optimization of Grid-Tied Microgrids Under Binomial Differentiated Tariff and Net Metering Policies: A Brazilian Case Study

Henry L. López-Salamanca¹ · Lúcia V. R. Arruda¹ · Leandro Magatão¹ · Julio E. Normey-Rico²

Received: 14 March 2018 / Revised: 22 June 2018 / Accepted: 23 July 2018 / Published online: 2 August 2018
© Brazilian Society for Automatics--SBA 2018

Abstract

Integration and coordinated operation of renewable energy sources (RESs) offer to conventional consumers the possibility to control energy production and consumption in order to obtain technical and economic benefits. In this work, a mixed-integer linear programming approach is proposed to model and optimize DC-coupled grid-tied microgrids. The objective is to reduce industrial consumer electricity bill and energy storage systems degradation, considering operational constraints and rules defined by a complex binomial differentiated tariff and net metering policies to exchange energy. A novel model is developed to DC-coupling integration considering the efficiency of power transformation process and elements with two possible power flow conditions. An original formulation based on logical constraints is also proposed to model the net metering policies and to find the best compensation energy strategy for solving the optimization problem. A case study of a Brazilian industrial consumer, owner of a real-world DC grid-tied microgrid, is presented. The proposed approach involves low-cost procedures that can be integrated into a commercial solution to optimize microgrids in similar net metering contexts, encouraging the use of RESs in developing countries.

Keywords Renewable energy sources · Mixed-integer linear programming · Net metering policies · DC-coupled microgrids · Power management system

1 Introduction

In Brazil, the demographic and economic activity growing in last years has resulted in a constant increase in the electric energy consumption. Local studies show that the residential consumption represents a 10.5% of total energy consumption and, according to official projection, the residential consumption will increase from 105 TWh in 2010 to 283 TWh in 2030

(Januzzi and Augustos 2013). In this scenario, and in agreement with the worldwide objective of a clean and sustainable energy production, the use of renewable energy sources (RESs) by residential and industrial consumers has been introduced just recently in Brazil as a solution to energy supply, expanding and diversifying the country's electric power generation. The Brazilian government through the regulatory agency ANEEL has directed efforts to create conditions for the insertion of RESs. The normative resolution 687 (ANEEL 2015) provides incentives to grid-connected distributed generation by small producers and to introduce a net metering system. The net metering policies are interesting where grid parity exists. This is the Brazilian case where the residential tariffs are higher than 0.33 US\$/KWh, a large solar radiation resource is available, up to 2200 kWh/m²/year, and cost of a photovoltaic system (PV) is lower than 3333 US\$/kWp (Januzzi and Augustos 2013). For these reasons, the development of mathematical models improving grid parity and allowing the optimized insertion of distributed generators (DGs) and RES into Brazilian grid is a need.

The integration of DGs, RESs, ESSs (energy storage systems) and electrical loads constitutes a microgrid, which

✉ Henry L. López-Salamanca
henry@lactec.org.br

Lúcia V. R. Arruda
lvrrarruda@utfpr.edu.br

Leandro Magatão
magatao@utfpr.edu.br

Julio E. Normey-Rico
julio.normey@ufsc.br

¹ Federal University of Technology-Paraná, Av. Sete de Setembro, 3165, Curitiba, PR 80230-901, Brazil

² Federal University of Santa Catarina, C. Universitário Reitor João David Ferreira Lima, Florianópolis, SC 888040-900, Brazil

can operate connected with the grid or stand alone and can exchange energy with its energy suppliers. The coordinated operation of these microgrid elements and the development of optimization and control strategies for sizing and managing energy sources enhance their performance and make the entire system sustainable (Nehrir et al. 2011).

Majority of these strategies are devoted to AC-coupled grid-tied microgrids. However, with the significant increase in DC loads as notebooks, cell phones, LED lights, EVs, among others, the control and optimization of DC microgrids could be a viable economic solution for future energy needs. Some advantages of DC microgrids are the easier integration of DC RES as PV systems and fuel cells, ESSs and a more efficient supply of DC loads due to the reduction in multiple power converters (Lotfi and Khodaei 2017).

With these premises and since few studies have been reported considering the technical, economical and normative Brazilian context, this work proposes a mixed-integer linear programming (MILP) approach to model and solve the optimization problem of DC-coupled grid-tied microgrids under binomial differentiated tariff and net metering policies in the Brazilian context.

The proposed approach takes into account the development of a novel MILP electrical model, considering the balance between energy production and consumption at AC bus and DC bus, the efficiency of power transformation process, bidirectional power flow dispositives and analysing all possible power flow conditions. This new model prevents solutions contemplating simultaneous ESS charging and discharging, simultaneous power flow through power inverter (i.e. from DC bus to AC bus and vice versa), and purchasing and exporting energy from or to utility grid.

In fact, these simultaneous events are physically unrealizable and the developed models must assure a reachable solution. For this, some works in the literature use binary variables to control flow direction and schedule elements, and the resulting models demand a heavy computational time to reach solution due to its size. The works of Gambino et al. (2014) and Parisio et al. (2016) are examples of this solution. Both works develop MILP approaches using a mixed logical dynamical (MLD) framework to solve the cited problem in AC grid-tied microgrids, but the resulting models are cumbersome. An alternative is to develop simplified models encompassing only some microgrid conditions. This is the case of the MILP model proposed by Ravichandrad et al. (2018) to optimize AC grid-tied microgrids under feed-in policies, wherein an on/off control is used to charge electric vehicles (EVs). The solution limits the charge to a fixed power rate. Also, Yao and Venkatasubramaniam (2015) propose an integer linear programming (ILP) to optimize a community ESS under net metering policies. For this, the battery efficiency is assumed perfect and the energy levels are assumed discrete. That are unrealistic assumptions.

The MILP electrical model proposed in this paper overcomes the above-cited limitations and assumptions, due to the adopted formulation based on logical constraints, and the connection between binary and continuous variables is carried out without power and energy continuous value limitations. As a result, the proposed model demands lower computational resources and runs with an open-source software.

As commented above, the majority of power grid models are presently AC type; thus, only a small number of works consider DC and hybrid systems. Moreover, these works are mainly directed only to power management strategies (Nejabatkhah and Li 2015). The optimization problem of a DC grid-tied microgrid as approached in this work is not often addressed. As an example, we only cite two of them. Dufo-López et al. (2007) propose a genetic algorithm approach to optimize a stand-alone hybrid-coupled microgrid. Although the electrical model considers power converters efficiency and energy cycling cost through the ESS for a single charge rate, the optimization model solution by heuristic approaches does not guarantee an optimal solution and can consume time processing which could make an online control application unfeasible. In Bordons et al. (2015), the optimization problem of a DC grid-tied microgrid is solved by quadratic programming (QP). A detailed model that penalizes high ESS charge and discharge rates is proposed.

Adding to this context, the proposed model provides an alternative approach to optimize a DC grid-tied microgrid based on MILP.

Concerning net metering policies, the optimization and control solutions found in the literature are based on simplified tariffs and unrealistic net metering policies. Such is the case of Ratnam et al. (2015) that propose a linear programming (LP) approach to maximize the operational saving, when excess generation of PV and battery residential systems are balanced via net metering policy in which consumer is billed and compensated at same rate. In Fonseca et al. (2015), an if-then-else control is proposed for battery management of DC-coupled microgrids considering a monomial differentiated tariff that accounts just the energy consumption. The solution just defines the intervals that battery must be charged and discharged.

Our optimization model quantifies in a unified cost function the rules of a complex binomial differentiated tariff and the policies for energy exchange between consumer and utility grid defined by the complex Brazilian net metering system. This model also considers operational restrictions, different energy compensation strategies and the ESS degradation. Moreover, the set of necessary parameters for the ESS and overall microgrid elements modelling is taken from equipment basic technical information available by the manufactures.

The originality of the DC grid-tied optimization approached and the feasibility of the developed solution application in online control and management systems sum up the contribution of this work. Even though the proposed solution is applied to the Brazilian reality, it can be applicable to other countries with similar characteristics.

This paper is organized in five sections. After this introduction, the problem description is presented in Sect. 2, and the optimization model formulation is detailed in Sect. 3. In Sect. 4, simulation results are analysed. Finally, Sect. 5 summarizes and concludes this paper.

2 Problem Description

The MILP optimization approach proposed in this work considers DC-coupled grid-tied microgrids composed by RESs, electrical loads and ESSs. The proposed solution is evaluated for a real-world microgrid located in Curitiba/PR owned by a Brazilian industrial consumer. This DC-coupled microgrid can operate in stand-alone or grid-connected mode. The microgrid consists of a 30.36-kW_p photovoltaic (PV) system connected to a 48-V DC bus through a 34.56-kW and 97.5% efficiency charge controller set. A 63.36-kWh lead acid battery bank is directly connected to the DC bus. An inverter set of 32.4 kW total power and 93% efficiency connects the solar panels and the battery bank to AC bus. Copel Distribution S.A.—COPEL DIS S.A, a Brazilian electric utility to Paraná State, supplies the electrical energy for this consumer. The rules of the green tariff (ANEEL 2010), a binomial differentiated tariff, the net metering policies established by the normative resolution 687 (ANEEL 2015) and some commercial procedures drive the energy exchange between the microgrid and the electric utility.

Considering a microgrid hierarchical control framework (Palizban et al. 2014), the MILP model presented in this work corresponds to an embedded module of an online robust model predictive control (MPC) of a third-level power management system (PMS). In this control level, the power through the EES is the control signal and the power from/to utility grid is the process output. The power supplied by the RES and the power required by the electrical load are uncontrollable variables whose future values are estimated during a prediction horizon by the forecasting module also embedded in the PMS. At each iteration, the proposed model solves an optimization problem aiming to optimize the microgrid operation within safe limits, reducing the electricity bill and prolonging the ESS lifetime. The computed solution addresses just the microgrid operation, without dealing with the sizing problem.

The microgrid control implementation uses the AXS Port Modbus TCP of the Outback Power (for microgrid remote monitoring and control) as an interface between the PMS

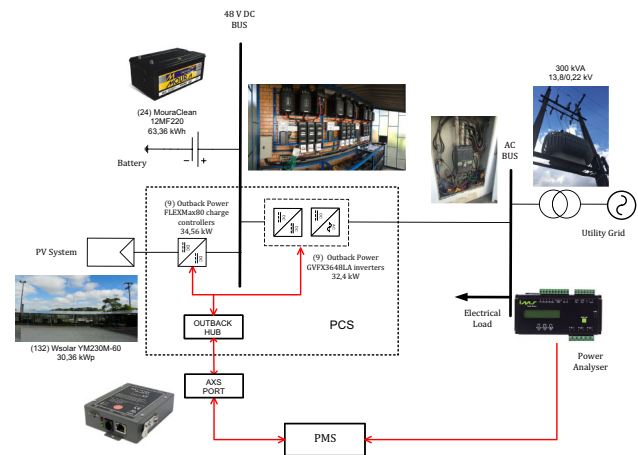


Fig. 1 Microgrid overview

and the microgrid power conversion system (PCS). Charge controllers, inverters and a hub for their communication and coordinated operation compose the PCS. Some PCS functions are maximum power point tracking (MPPT) for the PV system, control of ESS charge and discharge, voltage and frequency regulation, synchronization with the utility grid, control of output current harmonics and power factor.

From the API Development Kit available at the Outback Power website, a C program has been developed to access data registered by the PCS and to set the power converters configuration parameters. Therefore, from PV power output and electrical load power, registered by a power analyser, the PMS predicts future values (forecasting module), solves the optimization problem (MILP model module) and defines at each iteration the battery charge and discharge power set point (MPC) that is sent to the PCS.

Figure 1 shows the microgrid schematic overview including the electrical and the control diagrams.

This paper presents only the mathematical model that defines the proposed MILP approach and discusses computational validation results. The overall control solution development and its implementation is the aim of next works. For a better understanding of the problem, the next section details the green tariff, the net metering policies, the ESS energy cycling cost, the technical characteristics and the integration of microgrid elements in a DC-coupled configuration, including their respective mathematical models.

3 Optimization Model

Tables 3 and 4 from Appendix contain, respectively, all parameters and variables used in the optimization model.

As mentioned in the problem description, the controller objective is to optimize the microgrid operation, minimizing the price of electricity bill and prolonging the ESS lifetime.

These aspects are merged in the objective function described by Eq. (1).

$$\min(Z) = \alpha_D \tilde{Z}D(D_{\max}) + \alpha_E ZE(\text{PgS}(k), \text{PgC}(k)) + \alpha_{\text{ESS}} \tilde{Z}_{\text{ESS}}(\text{PBS}(k), \text{PBC}(k)) \tag{1}$$

where α_D, α_E and α_{ESS} are weighting factors used to prioritize the costs that compose the objective function, k corresponds to the day hour, $k \in \{1, \dots, N_y\}$ and N_y is the prediction horizon. $\tilde{Z}D$ is defined as function of D_{\max} and quantifies the demanded and exceeding power price in the green tariff context. ZE depends on the power from $\text{PgS}(k)$ and to $\text{PgC}(k)$ utility grid and quantifies the energy price under net metering policies. \tilde{Z}_{ESS} is the cost of cycling energy through the ESS, and it depends on ESS discharge power $\text{PBS}(k)$ and charge power $\text{PBC}(k)$. \tilde{Z} denotes the piecewise-linear Sherali formulation approximation (Sherali 2001). Each of these costs, including the Sherali formulation, is detailed in Sects. 3.1–3.3.

3.1 Demanded and Exceeding Power Price

In Brazil, the ANEEL normative resolution 414 establishes general conditions for electricity supply. The explanation of the tariffs, the guidelines for the contracts, the measurement for billing are topics addressed in this resolution (ANEEL 2010).

The green tariff, addressed in this work, is a binomial differentiated tariff, i.e. billing of power demand (R\$/kW) and billing of active electric energy consumption (R\$/kWh). The bill considers price for total consumed energy and for power demand during the billing period.

Relative to energy consumption price, there are two tariffs for energy consumption defined by two hourly intervals, peak and off-peak periods. The peak period consists of three consecutive hours per day when maximum energy prices are applied.

Relative to power demand price, there is a single tariff for power demand and there are three possible demanded power conditions. Equations (2)–(4) describe these conditions:

Condition 1: $D_{\max} > D_{\text{lim}}$

$$ZD = D_{\max} T D_1 + (D_{\max} - D_{\text{cont}}) T E_x \tag{2}$$

Condition 2: $D_{\text{cont}} \leq D_{\max} \leq D_{\text{lim}}$

$$ZD = D_{\max} T D_1 \tag{3}$$

Condition 3: $D_{\max} < D_{\text{cont}}$

$$ZD = D_{\max} T D_1 + (D_{\text{cont}} - D_{\max}) T D_2 \tag{4}$$

The price of power demand ZD is a discontinuous function defined by three regions, according to Eqs. (2)–(4). The Sherali formulation (Sherali 2001) is used for including the tariff components relative to demand price and penalty for exceeding the contracted power in the objective function. Equations (5)–(9) describe the constraints for the discontinuous piecewise-linear function:

$$D_{\max} = \sum_{i=1}^{r_{ZD}} [D_{\max i-1} \lambda_i^L + D_{\max i} \lambda_i^R] \tag{5}$$

$$\tilde{Z}D(D_{\max}) \approx \sum_{i=1}^{r_{ZD}} [ZD(D_{\max i-1}) \lambda_i^L + ZD(D_{\max i}) \lambda_i^R] \tag{6}$$

where:

$$\lambda_i^L + \lambda_i^R = y_i \quad \forall i = 1 \dots r_{ZD} \tag{7}$$

$$\sum_{i=1}^{r_{ZD}} y_i = 1 \tag{8}$$

$$\lambda_i^L, \lambda_i^R \in \mathbb{R}_+ \quad \forall i = 1 \dots r_{ZD} \tag{9}$$

$$y_i \in \{0, 1\} \quad \forall i = 1 \dots r_{ZD}$$

For power demand price, r_{ZD} is equal to three, $D_{\max i}$ corresponds to maximum power values defined between operational system bounds, and $\tilde{Z}D \approx ZD$ is calculated by the optimization model just one time for all bill period and for minimizing the power demand price. The continuous variables λ_i^L, λ_i^R and the binary variables y_i are decision variables defined by the optimization model just one time, too. Figure 2 illustrates the linearized price of power demand ZD .

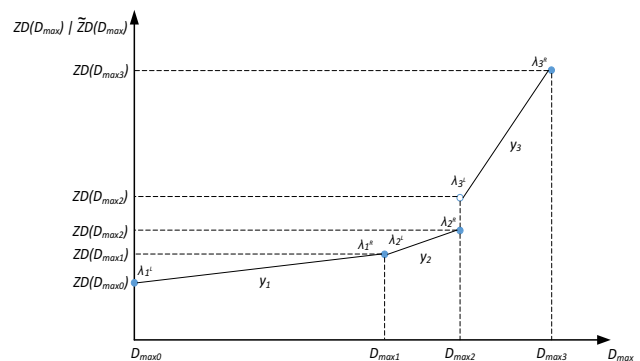


Fig. 2 Price of power demand discontinuous piecewise-linear function

Table 1 Logical relations for defining a compensation strategy attending net metering policies

Statement			Logical propositions	Str.	Compensation strategy equation
δ_{OP}	δ_P	δ_C			
0	0	0	$(1 - \delta_{OP}) \wedge (1 - \delta_P) \wedge (1 - \delta_C) = \delta_{z1}$	Z1	$E1 = \Sigma PgS_{OP}T_{OP} - \Sigma PgC_{OP}T_{AOP} + \Sigma PgS_P T_P - \Sigma PgC_P T_{AP}$
1	0	0	$\delta_{OP} \wedge (1 - \delta_P) \wedge (1 - \delta_C) = \delta_{z2}$	Z2	$E2 = \Sigma PgS_{OP}(T_{OP} - T_{AOP}) + \Sigma PgS_P T_P - (\Sigma PgC_P - \Delta OPt_{opp})T_{AP}$
0	1	0	$(1 - \delta_{OP}) \wedge \delta_P \wedge (1 - \delta_C) = \delta_{z3}$	Z3	$E3 = \Sigma PgS_{OP}T_{OP} - (\Sigma PgC_{OP} - \Delta Pt_{pop})T_{AOP} + \Sigma PgS_P (T_P - T_{AP})$

3.2 Net Metering Policies Model

In Brazil, the net metering policies are established by the normative resolution 687 (ANEEL 2015). Net metering allows electricity consumers to use the energy surplus, which is exported to the utility grid, as energy credits. These credits can be used for a 60-month period by the consumer unit, or another unit of the same ownership, to reduce the energy consumption price of its electricity bill. If the consumer unit produces less energy than the consumed, it should pay just the difference. Otherwise, the consumer will receive this “energy credit” at the next month electricity bill.

For differentiated tariff as green tariff, when the active energy produced by the consumer is higher than the consumed energy in an hourly interval (e.g. off-peak), the difference should be used for compensating the energy consumption in other hourly interval (e.g. peak), using an adjustment factor, but at the same billing cycle. Accomplishing this, if energy credits still exist, the utility grid has to inform at the electricity bill the energy credits (kWh) at each hourly interval to be used at the subsequent cycle.

The proposed approach models and includes the Brazilian net metering policies as described above, in a unified objective function. All possible conditions for energy exchange between the utility grid and the consumer are modelled by means of logical relations as presented in Table 1. The energy exchange is limited to consumption of “energy credits” at same month and at same consumer unit.

In Table 1, tariffs T_{AOP} and T_{AP} are annually authorized by ANEEL for each energy utility and tariffs T_{OP} and T_P are final tariffs applied by energy utilities including taxes.

The strategies Z1 to Z3 are defined using a set of MILP expressions that represents logical constraints in the implication form (LCIF). In these expressions, the continuous variables are defined by Eqs. (10)–(13). Considering a sample rate of 1 h for the optimization model formulation, there exists equivalence between the energy and the power sum for the bill period.

$$\Delta OP = \Sigma PgS_{OP} - \Sigma PgC_{OP} \tag{10}$$

$$\Delta P = \Sigma PgS_P - \Sigma PgC_P \tag{11}$$

$$\Delta C1 = \Delta OPt_{opp} + \Delta P \tag{12}$$

$$\Delta C2 = \Delta OP + \Delta Pt_{pop} \tag{13}$$

The energy consumption and net metering policies are finally included in the objective function by Eqs. (14) and (15). Constraint (15) enforces the condition that just one compensation strategy must be considered in the problem solution. The optimization model decides the best strategy for minimizing the energy price for the billing period.

$$ZE = \sum_{j=1}^3 Z_j \tag{14}$$

$$\sum_{j=1}^3 \delta_{Z_j} = 1 \tag{15}$$

3.3 Cost of Cycling Energy Through ESS

The adopted quantification of cycling energy through the ESS (Z_{ESS}) is based on (Dufo-López et al. 2007; Bordons et al. 2015; Garcia-Torres et al. 2016). This formulation considers charging and discharging processes and penalizes high currents through the ESS using the Peukert’s coefficient (Peukert 1897).

For solving the optimization problem by a MILP approach, the corresponding exponential equation is linearized $\tilde{Z}_{ESS} \approx Z_{ESS}$ using the Sherali formulation (Sherali 2001) as indicated in Eq. (16):

$$\tilde{Z}_{ESS} = \sum_{k=1}^{N_y} \left[\tilde{Z}_{ESS_s}(\text{PBS}(k))K_{dis} + \tilde{Z}_{ESS_c}(\text{PBC}(k))K_{ch} \right] \tag{16}$$

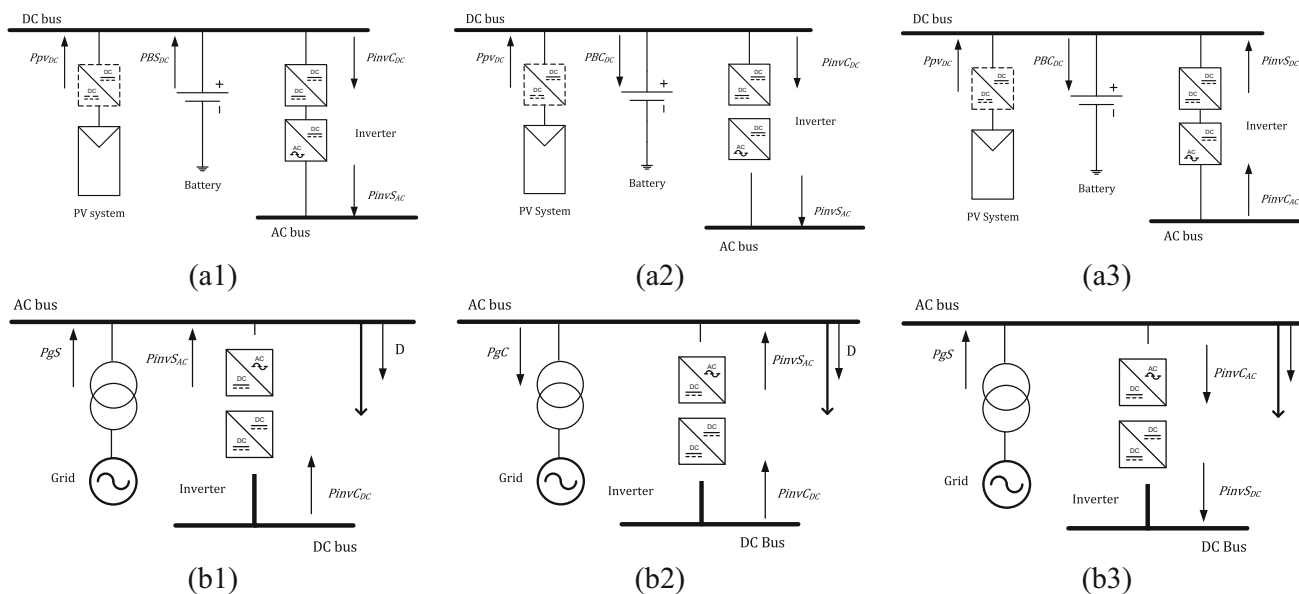


Fig. 3 Schematic diagram of DC-coupled grid-tied microgrid including different power flow conditions

where \tilde{Z}_{ESS_S} ($PBS(k)$) and \tilde{Z}_{ESS_C} ($PBC(k)$) are, respectively, the piecewise-linear functions for the discharging and charging processes, calculated at each hour. K_{dis} and K_{ch} are discharging and charging constants.

The set of necessary parameters to quantify the cost of cycling energy through the ESS are easily calculated from manufacturer's available information (for a new ESS) or simple charging tests (for a used ESS).

3.4 Constraints

As hereafter indicated by expressions (2)–(16), a set of constraints were already included in the model, involving: constraints relative to linearization using the Sherali formulation for the demanded power price and for the cost of cycling energy through the ESS, and the constraints relative to energy price and energy compensation policies. However, physical limits to guarantee the microgrid operation within safe limits must be also included. For instance, ESS safe operation constraints, including maximum power that can be supplied or consumed by the ESS, maximum and minimum amount of energy, and constraints that guarantee at each iteration just one condition for ESS (charging or discharging), are included in the model. For that, ESS model is used which is reported in the works (López-Salamanca et al. 2014; Fonseca et al. 2015; Bordin et al. 2017) and the software (HOMER Energy 2015).

Furthermore, constraints relative to microgrid elements integration at the DC-coupled bus and their operation in grid-connected mode must be also included.

3.4.1 Electrical Model

The different power flow configurations at DC-coupled grid-tied microgrids, as shown in Fig. 3, must also be considered into optimization model. For this, the production and consumption energy balance at DC bus and AC bus is analysed for all possible power flow conditions.

Figure 3a describes the power flow at DC bus for three possibilities: (a1) PV system and ESS are supplying power to the DC bus, and the equivalent power is supplied to the AC bus through the DC/AC inverter; (a2) as the previous case, just with the difference that the ESS is now charging; and (a3) PV system and utility grid through the AC/DC inverter are supplying power at DC bus, for ESS charging.

Figure 3b describes the power flow at AC bus for the next possibilities: (b1) utility grid is supplying power to the AC bus, load is requiring power, and the DC bus is supplying power to the AC bus through the DC/AC inverter; (b2) the DC bus is supplying power to the AC bus through the DC/AC inverter, and this power is higher than the power required by the load; for that reason, the surplus power is exported to the utility grid; (b3) is similar to (b1) with the difference that ESS is charging by the utility grid through the AC/DC inverter. The DC/AC inverter is the same as the AC/DC inverter. The nomenclature is only adopted to specify the flow direction (from/to).

Finally, the novel MILP electrical model for optimization and control solutions of DC-coupled grid-tied microgrids can be completed. All power flow conditions at DC bus and AC bus described in Fig. 3 are considered, and other electrical constraints (Eqs. 17–44) are included in this model. These constraints are described in the following. All the continuous

variables of the proposed model are defined as positive, i.e. $\in \mathbb{R}_+$.

At each iteration, the battery is either charging or discharging, guaranteed by constraints (17)–(19).

$$\delta_{BS}(k) + \delta_{BC}(k) = 1 \tag{17}$$

$$PBS(k) \leq \delta_{BS}(k)M \tag{18}$$

$$PBC(k) \leq \delta_{BC}(k)M \tag{19}$$

Equations (20)–(24) consider the efficiencies of power converters and battery charging and discharging efficiencies.

$$P_{PVDC}(k) = \eta_{PV} P_{PV}(k) \tag{20}$$

$$PBS_{DC}(k) = \eta_{dB} PBS(k) \tag{21}$$

$$PBC_{DC}(k) = \eta_{cB}^{-1} PBC(k) \tag{22}$$

$$PinvS_{DC}(k) = \eta_{inv\ AC/DC} PinvC_{AC}(k) \tag{23}$$

$$PinvC_{DC}(k) = \eta_{inv\ DC/AC}^{-1} PinvS_{AC}(k) \tag{24}$$

Equations (25) and (26) guarantee the balance between the energy produced and consumed at DC bus and AC bus, respectively.

$$PBS_{DC}(k) + P_{PVDC}(k) + PinvS_{DC}(k) = PBC_{DC}(k) + PinvC_{DC}(k) \tag{25}$$

$$PgS(k) + PinvS_{AC}(k) = PgC(k) + D(k) + PinvC_{AC}(k) \tag{26}$$

The power is flowing from either the DC bus to the AC bus or the AC bus to DC bus. This condition is assured by constraints (27)–(29) at DC bus, and (30)–(32) at AC bus, and reinforced by constraints (33) and (34).

$$\delta_{IS_{DC}}(k) + \delta_{IC_{DC}}(k) = 1 \tag{27}$$

$$PinvS_{DC}(k) \leq \delta_{IS_{DC}}(k)M \tag{28}$$

$$PinvC_{DC}(k) \leq \delta_{IC_{DC}}(k)M \tag{29}$$

$$\delta_{IS_{AC}}(k) + \delta_{IC_{AC}}(k) = 1 \tag{30}$$

$$PinvS_{AC}(k) \leq \delta_{IS_{AC}}(k)M \tag{31}$$

$$PinvC_{AC}(k) \leq \delta_{IC_{AC}}(k)M \tag{32}$$

$$\delta_{IS_{AC}}(k) + \delta_{IS_{DC}}(k) = 1 \tag{33}$$

$$\delta_{IC_{AC}}(k) + \delta_{IC_{DC}}(k) = 1 \tag{34}$$

The last constraints prevent solutions with simultaneous bidirectional power flow through the power inverter. In particular, constraints (35)–(37) guarantee the utility grid is supplying power to AC bus or the surplus power is exported to utility grid.

$$\delta_{gS}(k) + \delta_{gC}(k) = 1 \tag{35}$$

$$PgS(k) \leq \delta_{gS}(k)M \tag{36}$$

$$PgC(k) \leq \delta_{gC}(k)M \tag{37}$$

Inequalities (38) and (39), (40) and (41) limit the inverter power output at AC side and DC side.

$$PinvS_{DC}(k) \leq Pinv_{maxDC} \tag{38}$$

$$PinvC_{DC}(k) \leq Pinv_{maxDC} \tag{39}$$

$$PinvS_{AC}(k) \leq Pinv_{maxAC} \tag{40}$$

$$PinvC_{AC}(k) \leq Pinv_{maxAC} \tag{41}$$

Inequalities (42) and (43) limit the power supplied by or exported to the utility grid, respectively.

$$PgS(k) \leq P_{maxGS} \tag{42}$$

$$PgC(k) \leq P_{maxGC} \tag{43}$$

In this electrical model, a Big-M formulation allows the logical connection between the binary variables with the continuous variables within constraints (18) and (19), (28) and (29), and (36) and (37), respectively.

Finally, inequality (44) allows computing the maximum active power demanded without losing the model linearity.

$$PgS(k) \leq D_{max} \tag{44}$$

4 Results and Analysis

The developed model is validated through computational simulations based on real-world data from the microgrid described in Sect. 2.

Figure 4 shows the consumer load and power PV system profile considered for simulations. In this figure, the label Load also corresponds to a consumer without the microgrid and the label Load+RES is a consumer with RES. COPEL DIS S.A. establishes the peak interval from 6 p.m. to 9 p.m. and the off-peak interval to the complementary daily period. The contracted power is 30 kW (green dashed line) and the limit power 31.5 kW (red dashed line).

Seven scenarios are simulated for a 24-h interval. The results allow to assert the economic benefits of the proposed model use and to validate this model.

Figure 5 shows the equivalent power at AC bus obtained for the following scenarios:

- Load+ESS: consumer with ESS,
- Load+RES+ESS: solution considering the overall cost function Z in Eq. (1),
- Load+RES+ESS ($\alpha_D = 0$): $\tilde{Z}D$ is not included into cost function Z ,

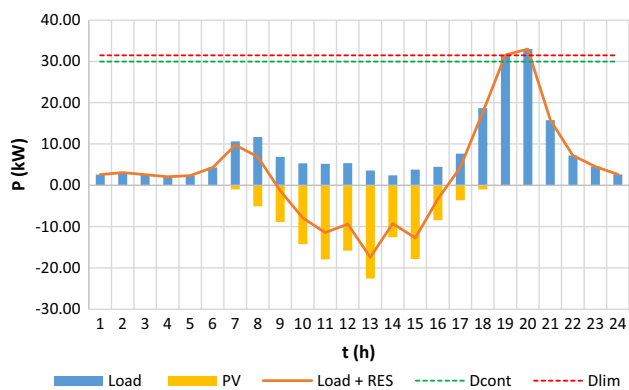


Fig. 4 Expected consumer load and power supplied by the PV system (Color figure online)

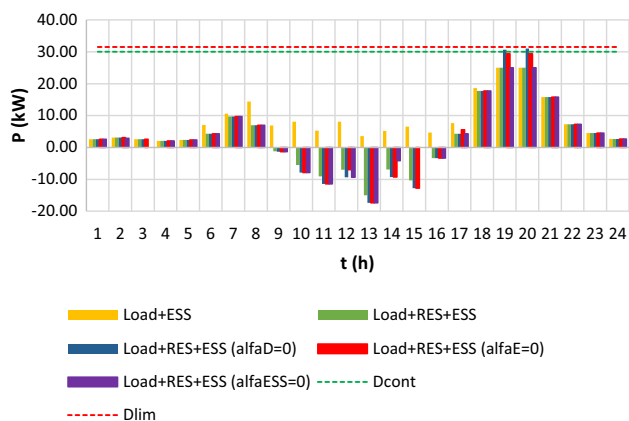


Fig. 5 Power at AC bus for scenarios with all the microgrid elements (Color figure online)

- Load + RES + ESS ($\alpha_E = 0$): ZE is not included into cost function Z,
- Load + RES + ESS ($\alpha_{ESS} = 0$): \tilde{Z}_{ESS} is not included into cost function Z.

Load and Load + RES scenarios are used only as reference for comparative analysis, and their equivalent power at AC

bus is given in Fig. 4. In this work, the simulation results analysis does not intend to evaluate the financial return of each option and just aims to show the economic advantages that could be obtained if the proposed solution is adopted. An interesting study, computing the battery payback and the total system payback for different battery depths of discharge scenarios when used an if-then-else control in the same microgrid used here, can be found in Fonseca et al. (2015).

The proposed optimization model is solved using the open-source LP/MILP integrated development environment GUSEK (2014). For an Intel® Core™ i5 CPU, 6 GB memory RAM, the processing time necessary to achieve the optimal solution for the overall cost scenario was around 2.55 s.

Table 2 presents the economic comparison of these scenarios.

For the Load+RES scenario, the energy surplus (i.e. energy produced by the PV system is higher than energy consumed by the load) at off-peak period is used to compensate the energy consumption at peak period. The price relative to power demand is the same obtained for the Load scenario, because D_{max} occurs at 8 p.m. (see Fig. 4) when there is no PV power production. In this scenario, an 8.72% reduction is achieved.

A better reduction, 17.12%, is obtained, only replacing the RES by the ESS in the proposed optimization model. This scenario uses the Z1 strategy from Table 1. Power purchased from utility grid is used for charging the battery at off-peak period when energy is low priced and used later to compensate the energy consumption at peak period (ZEP) when energy is more expensive. This condition reduces D_{max} and, therefore, the power demand price ZD. A cost relative to cycling energy through the ESS (Z_{ESS_S} plus Z_{ESS_C}) appears due to the ESS charge and discharge.

All the other scenarios consider the microgrid formed by all its elements (Load + RES + ESS).

Table 2 Economic comparison

	Load	Load+RES	Load+ESS	Load+RES+ESS (alfaD=0)	Load+RES+ESS (alfaESS=0)	Load+RES+ESS (alfaE=0)	Load+RES+ESS
ZE OP (R\$)	59.51	11.60	68.20	11.60	14.83	11.82	15.08
ZE P (R\$)	132.29	127.91	109.26	123.49	107.78	121.11	107.78
ZD (R\$)	407.58	407.58	297.64	324.70	297.64	311.54	297.64
Z ESS S (R\$)	0.00	0.00	14.09	1.80	16.08	4.27	14.09
Z ESS C (R\$)	0.00	0.00	7.56	0.00	14.60	1.93	7.56
Z (R\$)	599.38	547.09	496.75	461.59	450.94	450.67	442.15
Reduction (%)	0.00	8.72	17.12	22.99	24.77	24.81	26.23

The scenario with $\alpha_D = 0$ corresponds to Z2 choice in Table 1. The energy surplus at off-peak period is used to compensate the consumption at peak period. In this case, the power demand price is not penalized, and for that reason, D_{\max} and consequently ZD are the highest values when compared with the other scenarios computed by MILP model. Nevertheless, a higher reduction 22.99% is obtained, if compared with the Load+ESS scenario.

For $\alpha_{\text{ESS}} = 0$, the chosen strategy is Z1. The energy cycling cost through the ESS is not penalized and consequently Z_{ESS} presents the highest value. However, a higher compensation is obtained for peak period and a 24.77% total reduction is achieved.

Compared with the discussed scenarios, a better performance, 24.81% reduction, is obtained considering $\alpha_E = 0$. In this scenario, the chosen strategy is again Z2.

Finally, the best performance is obtained when all the components of the objective function are considered. In this case, the chosen strategy is Z1. A total of 26.23% reduction is achieved.

The results show that the best option for the consumer is to store in the ESS the energy produced by the PV system at off-peak period for later use at peak period when energy is more expensive and not to export it. This is explained by the net metering policies and mainly by the utility commercial procedures framework of the microgrid under study. The energy credits are computed from the surplus energy to be exported to utility grid using a non-tax tariff. Since the non-tax tariff is lower than tariff including taxes, a few energy credits are obtained if compared with the amount of exported energy.

In addition to the positive impact on the energy cost caused by stored energy for later use, the power demand that occurs at peak period is also reduced. This cost is not covered by energy credits because they are only applied for energy compensation.

The described previous impacts are possible when using a controllable ESS; for that reason, the scenarios with ESS have a better performance compared with the PV system scenario.

The comparative analysis and the previous discussion show that the proposed MILP approach is able to model the technical and commercial microgrid operation conditions and to define the better energy compensation strategy for reducing the electricity bill under these conditions. Therefore, the proposed solution is validated.

5 Conclusions

A mixed-integer linear programming (MILP) approach has been proposed and detailed to model DC-coupled microgrids based on balance between energy production and consumption at AC and DC bus, considering the efficiency of power transformation process. An optimization model using con-

tinuous and binary variables combined by mathematical and logical relations was developed to guarantee the correct microgrid operation and the adequate objective function formulation. The model prevents solutions contemplating simultaneous ESS charging and discharging; simultaneous power flow through power inverter (i.e. from DC bus to AC bus and vice versa); and purchasing and exporting energy from or to utility grid. This MILP formulation was fundamental to model all possible energy compensation strategies defined by net metering policies into a unified cost function. For this, it was necessary to quantify separately the net energy exported and consumed at each hourly interval, condition attended in a simple and original way using independent variables for each condition. Furthermore, this MILP approach allowed modelling the rules of a complex binomial differentiated tariffs that accounts for energy consumption, power demanded and penalties.

A case study of a Brazilian industrial consumer owner of a DC grid-tied microgrid is presented. From technical specifications of the microgrid and the rules of green tariff and the net metering policies defined by Brazilian normative resolutions, the proposed MILP model was solved using an open-source software and computationally validated for different simulated scenarios. The simulated results are presented only for a 1-day interval, but the proposed model can be extended for a 1-month interval, if load profile data and PV power supply data for this period are known.

The developed framework involves low-cost (or even cost-less) procedures and a very low processing time for minimal hardware requirements. These are relevant aspects aiming at the development of commercial solutions to optimize the operation of microgrids, encouraging the use of alternative energy distributed generation sources in developing countries, as Brazil.

Further studies will be carry out for embedding this offline MILP approach in an online robust MPC control to improve the microgrid performance. Complementary, efforts are being addressed to implement a power management system (PMS) based on the proposed MILP and the MPC control approach.

Acknowledgements Technical support from the Institute of Technology for Development—LACTEC is gratefully acknowledged. The authors also acknowledge CNPq, Grants 305816/2014-4, 401126/2014-5, 305785/2015-0 and 406507/2016-3 and CAPES, PDSE program, process 88881.135220/2016-01.

Appendix

Parameters and variables for the proposed MILP approach optimization model are presented in Tables 3 and 4, respectively. Dimensional values are between parentheses.

Table 3 Parameters

Parameters	Description
D_{cont}	Contracted active power (kW)
D_{lim}	Upper limit active power (kW)
M	Parameter used for the Big-M formulation (kW)
$P_{invmaxAC}$	Maximum inverter active power output at AC side (kW)
$P_{invmaxDC}$	Maximum inverter active power output at DC side (kW)
P_{maxGC}	Maximum active power exported to the utility grid (kW)
P_{maxGS}	Maximum active power purchased from the utility grid (kW)
TD_1, TD_2, TE_x	Tariffs relative to power demand and penalty for exceeding contracted power (R\$/kW)
T_{OP}, T_{AOP}	Tariffs relative to consumed energy at off-peak period (R\$/kWh)
T_P, T_{AP}	Tariffs relative to consumed energy at peak period (R\$/kWh)
t_{pop}, t_{opp}	Adjustment factor when there is energy compensation between different periods (dimensionless)
η_{cB}, η_{dB}	Storage charging and discharging efficiencies (dimensionless)
$\eta_{inv AC/DC}, \eta_{inv DC/AC}$	Inverter efficiency for power flow from AC bus to DC bus and DC bus to AC bus (dimensionless)
η_{PV}	PV system efficiency (dimensionless)

Table 4 Variables

Continuous variables	Description
D	Electrical load power (kW)
D_{max}	Maximum active power measured by the energy utility meter during the bill period (kW)
PBC	Battery charging power (kW)
PBC_{DC}	Battery charging power measured at DC bus (kW)
PBS	Battery discharging power (kW)
PBS_{DC}	Battery discharging power measured at DC bus (kW)
$P_{invC_{AC}}$	Power from AC bus to DC bus (kW)
$P_{invC_{DC}}$	Power from DC bus to AC bus (kW)
$P_{invS_{AC}}$	Power supplied at AC bus coming from DC bus (kW)
$P_{invS_{DC}}$	Power supplied on DC bus coming from AC bus (kW)
P_{gC}	Power exported to utility grid (kW)

Table 4 continued

Continuous variables	Description
P_{gS}	Power supplied by utility grid at AC bus (kW)
P_{PV}	Power supplied by the PV system (kW)
$Z1 \dots Z3$	Energy compensation strategies under net metering policies
$\Delta C1, \Delta C2$	Net energy when surplus energy at off-peak period is used to compensate energy consumption at peak period, and vice versa (kWh)
ΔOP	Difference between energy supplied by utility grid and energy exported by the consumer to utility grid, at off-peak period (kWh)
ΔP	Difference between energy supplied by utility grid and energy exported by the consumer to utility grid, at peak period (kWh)
λ^L, λ^R	Convex-combination weights of piecewise-linear function for power demand price (dimensionless)
$\Sigma P_{gC_{OP}}$	Total energy exported to utility grid at off-peak period (kWh)
ΣP_{gC_P}	Total energy exported to utility grid at peak period (kWh)
$\Sigma P_{gS_{OP}}$	Total energy supplied by the utility grid at off-peak period (kWh)
ΣP_{gS_P}	Total energy supplied by the utility grid at peak period (kWh)
<i>Binary variables</i>	
δ_{BC}	(1) Charging, (0) neutral mode of battery
δ_{BS}	(1) Discharging, (0) neutral mode of battery
δ_{gC}	(1) Surplus power at AC bus is exported to utility grid (0) neutral condition
δ_{gS}	(1) Utility grid supplying power to AC bus, (0) neutral condition
$\delta_{ICDC}, \delta_{ISAC}$	(1) Power from DC bus to AC bus, (0) neutral condition
$\delta_{ISDC}, \delta_{ICAC}$	(1) Power from AC bus to DC bus, (0) neutral condition
δ_C	(1) $\Delta C1 < 0$ and $\Delta C2 < 0$; (0) $\Delta C1 \geq 0$ and $\Delta C2 \geq 0$
δ_{OP}	(1) $\Delta OP < 0$; (0) $\Delta OP \geq 0$
δ_P	(1) $\Delta P < 0$; (0) $\Delta P \geq 0$
$\delta_{z1} \dots \delta_{z3}$	Used for defining a compensation strategy $Z1 \dots Z3$

References

- ANEEL. (2015). *Normative Resolution 687* (in portuguese). <http://www2.aneel.gov.br/cedoc/ren2015687.pdf>. Accessed 1 June 2018.
- ANNEEL. (2010). *Normative Resolution 414* (in portuguese). <http://www2.aneel.gov.br/cedoc/ren2010414.pdf>. Accessed 14 May 2015.
- Bordin, C., Anuta, H. O., Crossland, A., Gutierrez, I. L., Dent, C. J., & Vigo, D. (2017). A linear programming approach for battery degradation analysis and optimization in offgrid power systems with solar energy integration. *Renewable Energy*, *101*, 417–430.
- Bordons, C., García-Torres, F., & Valverde, L. (2015). Optimal energy management for renewable energy microgrids. *Revista Iberoamericana de Automática e Informática Industrial*, *12*, 117–132.
- Dufo-López, R., Bernal-Agustín, J. L., & Contreras, J. (2007). Optimization of control strategies for stand-alone renewable energy systems with hydrogen storage. *Renewable Energy*, *32*, 1102–1126.
- Fonseca, A. G., Langner, A. L., López-Salamanca, H., Siebert, L. C., Ferronato, F. A. S., Aoki, A. R., Alves, P., Riella R., et al. (2015). Building integrated photovoltaics for smart grids. In *Proceedings of 2015 IEEE PES innovative smart grid technologies Latin America*, Montevideo, Uruguay. <https://doi.org/10.1109/ISGT-LA.2015.7381267>.
- Gambino, G., Verrilli, F., Meola, D., Himanka, M., Del Vecchio, C., & Glielmo, L. (2014). Model predictive control for optimization of combined heat and electric power microgrid. In *Proceedings of the 19th IFAC World Congress*, Cape Town, South Africa. <https://doi.org/10.3182/20140824-6-ZA-1003.02354>.
- García-Torres, F., Valverde, L., & Bordons, C. (2016). Optimal load sharing of hydrogen-based microgrids with hybrid storage using model-predictive control. *IEEE Transactions on Industrial Electronics*, *63*, 4919–4928.
- GUSEK. (2014). *GLPK Under Scite Extended Kit*. <http://gusek.sourceforge.net/gusek.html>. Accessed 2 November 2014.
- HOMER Energy. (2015). *Global standard in microgrid software*. <http://www.homerenergy.com/index.html>. Accessed 13 July 2015.
- Januzzi, G., & Augustos, C. (2013). Grid-connected photovoltaic in Brazil: Policies and potential impacts for 2030. *Energy for Sustainable Development*, *17*, 40–46.
- López-Salamanca, H., Arruda, L., Magatão, L., & Normey-Rico, J. (2014). Using a MILP model for battery bank operation in the white tariff Brazilian context. In *Proceedings of the international renewable energy congress*, Hammamet, Tunisia. <https://doi.org/10.1109/TREC.2014.6826921>.
- Lotfi, H., & Khodaei, A. (2017). AC versus DC microgrid planning. *IEEE Transactions on Smart Grid*, *8*(1), 296–304.
- Nehrir, M. H., Wang, C., Strunz, K., Aki, H., Ramakumar, R., Bing, J., et al. (2011). A review of hybrid renewable/alternative energy systems for electric power generation: Configurations, control, and applications. *IEEE Transactions on Sustainable Energy*, *2*, 392–403.
- Nejabatkhah, F., & Li, Y. W. (2015). Overview of power management strategies of hybrid AC/DC microgrid. *IEEE Transactions on Power Electronics*, *30*, 7072–7089.
- Palizban, O., Kauhaniemi, K., & Guerrero, J. M. (2014). Microgrids in active network management—Part I: Hierarchical control, energy storage, virtual power plants, and market participation. *Renewable and Sustainable Energy Reviews*, *36*, 428–439.
- Parisio, A., Rikos, E., & Glielmo, L. (2016). Stochastic model predictive control for economic/environmental operation management of microgrids: An experimental case study. *Journal of Process Control*, *43*, 24–37.
- Peukert, W. (1897). Über die Abhängigkeit der Kapazität von der Entladestromstärke bei Bleiakкумуляtoren. *Elektrotechnische Zeitschrift*, *18*, 287–288.
- Ratnam, E. L., Weller, S. R., & Kellet, C. M. (2015). Scheduling residential battery storage with solar PV: Assessing the benefits of net metering. *Applied Energy*, *155*, 881–891.
- Ravichandrad, A., Sirouspour, S., Malysz, P., & Emadi, A. (2018). A chance-constraints-based control strategy for microgrids with energy storage and integrated electric vehicles. *IEEE Transactions on Smart Grid*, *9*, 346–359.
- Sherali, H. D. (2001). On mixed-integer zero-one representations for separable lower-semicontinuous piecewise-linear functions. *Operations Research Letters*, *28*, 155–160.
- Yao, J., & Venkatasubramanian, P. (2015). Optimal end user energy storage sharing in demand response. In *Proceedings of the 2015 IEEE international conference on smart grid communications*, Miami, USA. <https://doi.org/10.1109/SmartGridComm.2015.7436296>